Stagnation Pressure Effect on the Supersonic Two-Dimensional Plug Nozzle Design

HAMAIDIA Walid[1], *YAHIAOUI Toufik*[2], *ZEBBICHE Toufik*[2*]

1. Higher School of Aeronautical Techniques, Dar elbeida, Algiers, Algeria;
2. Institute of Aeronautics and Space Studies, University of Blida 1, BP 270 Blida 09000, Algeria

(Received 22 October 2022; revised 14 December 2022; accepted 14 January 2023)

Abstract: The aim of this work is to develop a new calculation program to study the stagnation pressure effect of the combustion chamber on the design of the supersonic two-dimensional plug nozzle giving a uniform and parallel flow at the exit section. The model is based on the use of the real gas(RG) approach. The co-volume and the intermolecular interaction effect are taken into account by the use of the Berthelot state equation. The molecular vibration effect is taken into account in our model to evaluate the behavior of the gas at high temperature. The stagnation pressure and the stagnation temperature are important parameters in our model. At the lip, the temperature and the density are given by the resolution of a two nonlinear algebraic equations, which are formulated by an integration of four complex functions. The resolution is made by a new, robust and a fast algorithm. The other parameters are determined by analytical relations. The flow expansion in the nozzle is of the Prandtl Meyer type. The nozzle contour determination is made by discretizing the expansion zone at the nozzle lip by several points. The Mach number, flow deviation, pressure, temperature and density parameters are determined after inversion of the two-variable Prandtl Meyer function. The integration of the functions presented in the calculation is made by the Gauss Legendre quadrature of order 30. The validation of the results is controlled numerically by the convergence of calculated critical sections ratio to that obtained by the theory, because the flow at the throat and the exit section is unidirectional. In this case, the nozzle contour and the flow parameters, like the mass of the nozzle, the length and the thrust coefficient converge automatically to the exact solution. Our new RG model is considered as a generalization to the two perfect gas (PG) and high temperature(HT) models. The two latter can make the design for low stagnation pressure, and do not give any information on the variation of the stagnation pressure. So if the latter is high, it is necessary to correct the results given by the PG and HT models by considering our developed RG model. The plug nozzle has better performances and design parameters compared to other existing nozzles like the minimum length nozzle(MLN). The mass, the length and the thrust coefficient of our plug nozzle for the PG and HT models are corrected by the use of our developed RG model. The application is made for air.

Key words: Berthelot state equation; Gauss Legendre quadrature; mass of the nozzle; minimum length nozzle (MLN); plug nozzle; Prandtl Meyer function; real gas (RG); stagnation pressure; stagnation temperature

CLC number: V925 **Document code:** A **Article ID:** 1005-1120(2023)01-0001-12

Notations

Ma	Mach number	α	Molecular vibration energy constant
x	Abscissa of the nozzle section	A	Section area
y	Radius of the nozzle section	ν_1	First part for Prandtl Meyer function
a	Constant of intermolecular forces	ν_2	Second part for Prandtl Meyer function
b	Constant of molecular size	ν	Prandtl Meyer function

*Corresponding author, E-mail address: z_toufik270169@yahoo.fr.

How to cite this article: HAMAIDIA Walid, YAHIAOUI Toufik, ZEBBICHE Toufik. Stagnation pressure effect on the supersonic two-dimensional plug nozzle design[J]. Transactions of Nanjing University of Aeronautics and Astronautics, 2023, 40(1): 1-12.

http://dx.doi.org/10.16356/j.1005-1120.2023.01.001

λ Throat length

N Descending Mach line number from the lip

t Integration variable

E_1 First function for Bernoulli equation

E_2 Second function for Bernoulli equation

V_S Sound velocity.

V Flow velocity

μ Mach angle

θ Flow angle deviation

P Pressure

T Temperature

R Gas constant

C_P Specific heat to constant pressure

C_F Thrust coefficient

C_T Specific heat at constant temperature

L Length of the nozzle

C_{Mass} Non-dimensional nozzle mass

γ Specific heats ratio

ρ Density

ε Tolerance of calculation (desired precision)

f_1, f_2 Nonlinear equations

PG Perfect gas model

HT High temperature model

RG Real gas model

PN Plug nozzle

PM Prandtl Meyer function

MLN Minimum length nozzle

NPR Nozzle pressure ratio

PDE Partial differential equation

ODE Ordinary differential equation

bar 1 bar$=1\times10^5$ Pa

Computed Calculated value

Exact Exact value

Indices

0 Stagnation condition (combustion chamber)

* Critical condition

E Exit section

j Point

F, G Throat of the nozzle

0 Introduction

In the aerospace industry, the problem of improving the performance of the supersonic nozzles plays a very important role. We are still interested in the nozzles giving a minimum length and mass with a high exit Mach number and thrust, to use the obtained gain for other physical considerations of the aerospace mission. So the search for the forms of the nozzle meeting this criterion is of current. The plug nozzle responds very well to this criterion.

The problem of controlling the flow behavior during the non-adaptation regime of the nozzle is topical, given the appearance of the side-loads causing in some cases explosions of the nozzle. Then the performances and the flow behavior of the gas are two very important factors and present problems of the news and future. The nozzle delivering maximum thrust is of great interest in aerospace propulsion. Nozzles responding to this criterion deliver a uniform and parallel flow to the exit section. The correct contour determination is made by using the Prandtl Meyer function giving complete expansion. The actual flow behavior depends on the stagnation parameters of the combustion chamber. The latter makes a chemical reaction under T_0 and P_0 conditions. Then the actual flow behavior depends on these two parameters. Therefore, the nozzle shape giving full expansion depends essentially on T_0 and P_0.

During the flight with altitude, the nozzle enters in the non-adaptation regime, or the flow depends on a very important parameter named by NPR. Here, the side-loads are observed in the nozzle. Its amplitude depends on NPR and the most important nozzle contour obtained during the design stage. To minimize the magnitude of the side-loads, it is considered that the supersonic nozzle must be redesigned by adding more P_0 than current assumptions.

In Refs.[1-5], the authors have studied the supersonic PN design on the calorically and thermally PG assumptions, without taking into account of T_0 and P_0 effect. Wind tunnel tests show that the results are acceptable for $Ma_E<2.00$ and $T_0<240$ K (if air is used) and no information on the value of P_0. This area does not reflect the current need for aerospace construction.

In Refs.[6-8], the author improved the research by taking into account the T_0 effect under the

threshold of molecules dissociation, called by HT model, without taking into account of P_0 again. Consequently they have widened somewhat the real scope of application ($Ma_E<5.00$, $T_0<3\ 550$ K for air), but no indication on the value of P_0. In this case, the authors have developed a new approach to the thermodynamic parameters at HT[7] and for PM at HT[9-10].

Refs.[11-13] provide verification of CFD flow in PN of Refs.[1-5] in the PG model frame. This study confirms the PN design results presented in Refs.[1-4] in the margin of Ma_E and T_0 previously discussed. Ref.[13] also represents a verification of the CFD flow in PN of Refs.[6-7] sized by HT.

The outside of adaptation studies presented in Ref.[14] demonstrate that there is a considerable formation of the side load in the nozzle according to the assumptions presented in Ref.[1-5], and Refs.[15-16] demonstrate that the side load according to the assumptions of Refs.[6-7] are rather less developed, because of the size of the nozzle is obtained according to the real flow behavior.

The various authors of the international aerospace engineering community have so far developed two models for the design of the various supersonic nozzles which are called by PG and HT models already discussed. The first reference to a new model for the calculation of supersonic flows for the purpose of making the design of supersonic nozzles is named by the RG model. Here the authors have explicitly added the effect of the stagnation pressure P_0 of the combustion chamber for internal flows, and of the ambient environment for external flows. So the first work, in this context, is that presented in Refs.[17-20]. In these references the authors first developed a model for the computation of the effect of P_0 on all the thermodynamic parameters in the supersonic regime, such as Ma, P/P_0, T/T_0, ρ/ρ_0; and A_E/A_* depending on T_0 and P_0 at the same time is a fairly large task. This work was followed by the work of the same authors presented in Refs.[17-18], where they presented the developments of the Prandtl Meyer function in the context of the RG model. This function in these two references depends again on the two parameters T_0 and P_0 in addition to the Mach number. In Refs.[9,21], the authors defined the PM functions for the models PG and HT which are as a fuction of the Mach number, and the specific heat ratio for the model PG, and a function of the Mach number, and of T_0 for the HT model. On the basis of these two old models on PM function, the authors developed models for the design of the plug nozzle as presented in Refs.[5-7].

In Ref.[22], a model based on the RG is developed in order to design a new contours for MLN of two-dimensional and axisymmetric geometries. Then a new model of MOC is developed in order to make the corrections on the contours of the same nozzles designed on the basis of the old PG and HT models, based on Ref.[21] for PG, and Refs.[23-24] for HT.

The aim of this work is to develop a new calculation program to study the stagnation pressure effect on the supersonic two-dimensional plug nozzle design by the determination of the contour of the nozzle numerically point by point to give a uniform and parallel flow at the exit section on the basis on a new RG model or real gas approach. The state equation for perfect gas $P=\rho RT$ is not valid in this case, where our interest is oriented to use the equation of state for RG. Here we have used the Berthelot state equation for its precision. Plus, all the relationships for the PG or HT models are not valid in our case. Then we must develop all relationship for RG model. The stagnation pressure and the stagnation temperature are important parameters in our RG model. At the lip of the throat, the values of T and ρ are given by a simultaneous resolution of a two nonlinear algebraic equations formulated by an integration of four complex functions. The resolution is made numerically by a robust and fast algorithm in high precision. The integration of the functions is made by the Gauss Legendre quadrature of order 30. Consequently, the values of θ, Ma, P are determined analytically. The validation of the results is controlled by the convergence of the critical sections ratio calculated numerically to that obtained by the theory, since the flow at the throat and the exit section are of uni-

directional and parallel flow. In this case, all the design parameters converge automatically to the exact solution. The design results can be compared and validated with the PG and HT models again, by taking low values of Ma_E, T_0 and P_0. The application is made for air.

1 Mathematical Formulation

Fig. 1 shows the two-dimensional PN with the presentation of the transition and the uniform regions to have a uniform and parallel flow at the exit section. The throat of the nozzle should be inclined with respect to the vertical to allow a horizontal flow to the exit section with fast flow expansion to have reduction in the length.

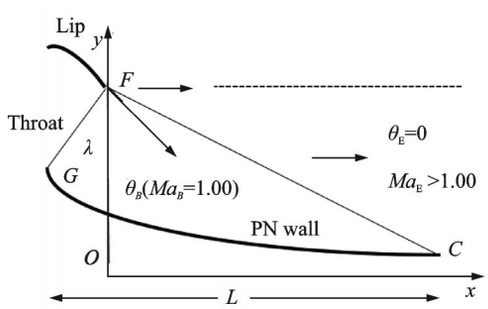

Fig.1 Flow field inside the supersonic two-dimensional PN giving a uniform and parallel flow at the exit section

In thermodynamics, all state parameters can be defined by two state variables[25-26]. In our study, T and ρ are chosen.

The flow through the nozzle is generated by the consideration of the PM's expansion. According to Refs.[17-18], the PM function is given by

$$\nu(T,\rho)=\int_{T}^{T_*}\nu_1(t,\rho)\mathrm{d}t+\int_{\rho}^{\rho_*}\nu_2(T,t)\mathrm{d}t \quad (1)$$

with

$$\nu_1(T,\rho)=\frac{\sqrt{Ma^2(T,\rho)-1}}{V^2(T,\rho)}C_P(T,\rho) \quad (2)$$

$$\nu_2(T,\rho)=\frac{\sqrt{Ma^2(T,\rho)-1}}{V^2(T,\rho)}C_T(T,\rho) \quad (3)$$

From the differential form Refs.[22-23], the Bernoulli equation can be written by

$$E_2(T,\rho)\mathrm{d}\rho=E_1(T,\rho)\mathrm{d}T \quad (4)$$

with

To have a uniform and parallel flow to the exit section, we must have the following condition

$$E_1(T,\rho)=\frac{C_P(T,\rho)}{V_S^2(T,\rho)} \quad (5)$$

$$E_2(T,\rho)=\frac{1}{\rho}-\frac{C_T(T,\rho)}{V_S^2(T,\rho)} \quad (6)$$

and

$$Ma(T,\rho)=\frac{V(T,\rho)}{V_S^2(T,\rho)} \quad (7)$$

$$\mu(T,\rho)=a\sin\frac{1}{Ma(T,\rho)} \quad (8)$$

The expressions of $V(T,\rho)$, $V_S^2(T,\rho)$, $C_T(T,\rho)$ and $C_P(T,\rho)$ are presented in Refs. [19-20].

The pressure can be calculated by the following Berthelot state equation[17-18, 25-26]

$$P(T,\rho)=\frac{\rho RT}{1-b\rho}-a\frac{\rho^2}{T} \quad (9)$$

For the PG and HT models, all the physical parameters can be determined according to a single variable, which can be chosen by the Mach number for the PG model, and the temperature for the HT model for numerical reason, respectively, while for our present RG model, all the thermodynamic parameters depend on two state variables which are T and ρ.

For air we have $\gamma_{PG}=1.402$, $R=287.102\ 9$ J/(kg·K), $a=117.266\ 6$ Pa·m^6, $b=1.073\ 34\times10^{-3}$ m^3 and $\alpha=3\ 056.0$ K[17-18, 25-26].

As the flow is 1D at the throat and the exit sections, Eq. (10) remains valid for the validation of the numerical obtained results[19-20].

$$\frac{A_E}{A_*}(\text{Exact})=\frac{y_A-y_C}{\lambda}=$$
$$\mathrm{Exp}\left(\int_{T_E}^{T_*}\frac{Ma^2(t,\rho_E)-1}{V^2(t,\rho_E)}C_P(t,\rho_E)\mathrm{d}t\right)\times$$
$$\mathrm{Exp}\left(\int_{\rho_E}^{\rho_*}\frac{Ma^2(T_E,t)-1}{V^2(T_E,t)}C_T(T_E,t)\mathrm{d}t\right) \quad (10)$$

Among several methods and techniques for evaluating the integral (10), we opt in our work, the quadrature of Gauss Legendre of order 40[27] because of its robustness in terms of speed of calculation and high precision. The abscissas and coefficients of Gauss Legendre's quadrature of order 40 can be found in Table 1.

Table 1 Abscissas and coefficients of the Gauss Legendre formulae of order 40

i	η_i	b_i
1	±0.038 772 417 506 050 821 933	0.077 505 947 978 424 811 264
2	±0.116 084 070 675 255 208 483	0.077 039 818 164 247 965 588
3	±0.192 697 580 701 371 099 716	0.076 110 361 900 626 242 372
4	±0.268 152 185 007 253 681 141	0.074 723 169 057 968 264 200
5	±0.341 994 090 825 758 473 007	0.072 886 582 395 804 059 061
6	±0.413 779 204 371 605 001 525	0.070 611 647 391 286 779 695
7	±0.483 075 801 686 178 712 909	0.067 912 045 815 233 903 826
8	±0.549 467 125 095 128 202 076	0.064 804 013 456 601 038 075
9	±0.612 553 889 667 980 237 953	0.061 306 242 492 928 939 167
10	±0.671 956 684 614 179 548 379	0.057 439 769 099 391 551 367
11	±0.727 318 255 189 927 103 281	0.053 227 846 983 936 824 355
12	±0.778 305 651 426 519 387 695	0.048 695 807 635 072 232 061
13	±0.824 612 230 833 311 663 196	0.043 870 908 185 673 271 992
14	±0.865 959 503 212 259 503 821	0.038 782 167 974 472 017 640
15	±0.902 098 806 968 874 296 728	0.033 460 195 282 547 847 393
16	±0.932 812 808 278 676 533 361	0.027 937 006 980 023 401 098
17	±0.957 916 819 213 791 655 805	0.022 245 849 194 166 957 262
18	±0.977 259 949 983 774 262 663	0.016 421 058 381 907 888 713
19	±0.990 726 238 699 457 006 453	0.010 498 284 531 152 813 615
20	±0.998 237 709 710 559 200 950	0.004 521 277 098 533 191 258

$$\theta_G = \nu_E = \nu(T_E, \rho_E) \tag{11}$$

The deviation of the lip from the vertical is given by $90^\circ - \theta_G$.

2 Calculation Procedure for the Lip

The problem is to calculate (T, ρ) at point A of the lip in Fig.1 by solving Eqs.(1,4) simultaneously. The values of Ma_3 and P_3 are determined by Eqs.(7, 9). The ratios T/T_0, ρ/ρ_0 and P/P_0 can then be determined.

Point F is a point of discontinuity. At this point, there is a sudden increase of all the thermophysical parameters. This discontinuity gives infinity of Mach line which will be from point F and reflected and absorbed by the wall of the nozzle as presented in Fig.2, because of the geometry is 2D. In each deviation, the flow angle and PM takes the following value

$$\theta_j = \theta_G - (j-1)\Delta\theta$$
$$j = 1, 2, 3, \cdots, N \tag{12}$$
$$\nu_j = \theta_G - \theta_j \tag{13}$$

For our calculation, we choose number N of descending Mach line from the lip F. Then, the step $\Delta\theta$ in Eq.(12) is given by

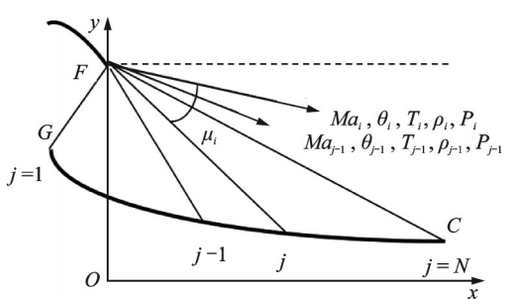

Fig.2 Wall point's illustration

$$\Delta\theta = \frac{\theta_G}{N-1} \tag{14}$$

The problem consists in determining T_j, ρ_j, Ma_j and P_j corresponding to this deviation number j. Since the function ν depends on two variables T and ρ. Then, we must solve simultaneously the two following nonlinear algebraic equations to obtain T_j and ρ_j.

$$f_1(T_j, \rho_j) = \nu(T_j, \rho_j) - \nu_j = 0 \tag{15}$$

$$f_2(T_j, \rho_j) = \int_{T_j}^{T_{j-1}} E_1(t, \rho_j)\mathrm{d}t - \int_{\rho_j}^{\rho_{j-1}} E_2(T_j, t)\mathrm{d}t = 0 \tag{16}$$

The values of Ma_j and P_j corresponding to this deviation number j, can be calculated by Eqs.(7,9) through replacing $T = T_j$ and $\rho = \rho_j$, respectively. It should be noted that $x_j = x_F$ and $y_j = y_F$.

The four integrals in Eqs.(15,16) are evaluated by Gauss Legendre formulae of order 40[27] to make fast computation with high precision (see Table 1).

The numerical techniques used to solve a system of nonlinear equations[27] are based on the Jacobean computation, which is formulated from the derivative of f_1 and f_2. The numerical tests by using these methods demonstrate that the determinant of this Jacobean (denominator of our computation of f_1 and f_2) takes a null value during the computation whatever the chosen initial vector is, which interrupts immediately the calculation. For this reason and to find a solution to our problem, we have developed fast and robust technique[28]. It converges towards the desired solution without failure.

3 Wall Contour

As the geometry is 2D, all the Mach lines chosen in the discretization that are derived from point F will be absorbed by the wall of the nozzle to give a uniform and parallel flow to the exit section, as shown in Fig.2. The flow in the zone FGC is of simple type and the lines joining the point F and the points of the wall are of straight lines.

To determine the position of the point j ($j=2, 3, \cdots, N$), we then develop equations connecting the points F and $j-1$ and the points F and j according to Fig.2. After solving the obtained equations, we obtain the positions (x_j, y_j) of the point j, by the following recursion relations

$$x_j = \frac{y_{j-1} - y_F - x_{j-1}\tan\theta_{j-1} + x_F\tan(\mu_j + \theta_j)}{\tan\theta_{j-1} - \tan(\mu_j + \theta_j)} \tag{17}$$

$$y_j = y_{j-1} - (x_j - x_{j-1})\tan\theta_{j-1} \tag{18}$$

The coordinates of point F are taken arbitrarily. In the calculations, we set $x_F=0.0$ and $y_F=1.0$. In Eqs.(17,18), a recursion formula has been obtained. So we need the first point when $j=1$. This point is point G given by

$$x_1 = x_G = x_F - \lambda\sin\theta_G \tag{19}$$

$$y_1 = y_G = y_F - \lambda\cos\theta_G \tag{20}$$

The properties θ_j, T_j, ρ_j, Ma_j and P_j at point j of the wall are the same as those obtained at points $j=1, 2, 3, \cdots, N$ of the lip F as the geometry is 2D.

During the transition from point $j-1$ to point j, there is an increase of the Mach number ($Ma_j > Ma_{j-1}$) and a decrease of θ, T, ρ and P, that is to say, $\theta_j < \theta_{j-1}$, $T_j < T_{j-1}$, $\rho_j < \rho_{j-1}$ and $P_j < P_{j-1}$.

At the end, the critical sections ratio corresponding to the chosen discretization will be given by

$$\frac{A_E}{A_*}(\text{Computed}) = \frac{y_F - y_N}{\lambda} \tag{21}$$

Once the convergence is reached, the design parameters L, C_{Mass}, C_F and all the thermodynamics parameters converge automatically towards the desired physical solution.

For the PG model[1-5], the design data are Ma_E and γ of the gas. For the HT model[6-7], the design data are Ma_E, T_0 and $C_P(T)$ of the gas; while for our RG model, the design data are extended to Ma_E, T_0, P_0 and $C_P(T, \rho)$ and $C_T(T, \rho)$ of the gas. Then, we can consider that the PG[1-5] and HT[6-7] models are special and particular cases of our presented RG model. In other words, our RG model is a generalization of the PG and HT models. The model PG can be obtained from our model RG when we take $a=b=\alpha=0$, and the HT model can be determined from RG when $a=b=0$. For the PG and HT models, Berthelot's state equation of the real gas becomes the state equation of perfect gas ($P=\rho RT$).

4 Results and Discussion

The presented design results are the nozzle shape and the numerical design parameters L/λ, C_{Mass}, C_F and A_E/A_* and the error caused by the PG and HT models compared to our RG model. All these five parameters depend essentially on Ma_E, T_0, P_0 and the chosen gas ($C_P(T, \rho)$, a, b and α).

4.1 Effect of P_0 on the design parameters

Figs.3,4 show the effect of P_0 on the contour of the two-dimensional PN, giving $Ma_E=3.00$ when $T_0=2\,000$ K. Six values of P_0 are taken which are 1.0 bar, 5.00 bar, 10.0 bar, 50.0 bar, 100.0 bar and 500 bar. The contours for the same data for PG[1-5] and HT[6-7] models are added for comparison purposes. The corresponded numerical design results are presented in Table 2. The influence of P_0

on the nozzle contour and on all the design parameters is clearly visible. The size of the nozzle given by our model RG is quite large compared to the size of the nozzles given by the PG and HT models, whatever the value of P_0 is. This result is very advantageous making it possible to say that in order to have a complete expansion inside the nozzle according to the real gas flow behavior, a large space of the nozzle is required compared to that given by the PG and HT models. These two models reduce the shape of the nozzle relative to the actual need for the gas flow behavior. For this reason the influence of P_0 is remarkable in all the design parameters.

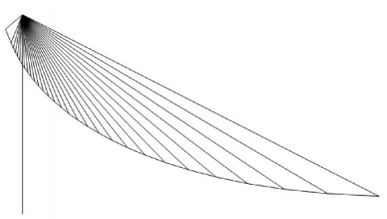

Fig.3 Mesh in two-dimensional PN

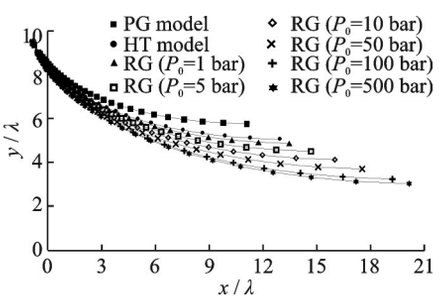

Fig.4 P_0 effect on the RG two-dimensional PN design (T_0=2 000K, Ma_E=3.00)

Table 2 Design values for the nozzles in Fig.4

N	P_0/bar	L/λ	C_{Mass}	C_F	A_E/A_*
1	1	16.745	18.192	0.991	5.594
2	5	16.763	18.211	0.855	5.595
3	10	16.784	18.233	0.855	5.596
4	50	16.888	18.339	0.850	5.608
5	100	17.116	18.578	0.851	5.621
6	500	18.099	19.582	0.825	5.702
7	PG[3]	12.698	13.594	0.746	4.220
8	HT[6]	14.949	16.142	0.884	4.995

It is estimated that the existence of side loads during the out-of-adaptation regime in our nozzle designed on the RG model will be reduced compared to that given by the HT and PG model, and will be justified by the wind tunnel tests.

If the HT model is used to determine the flow parameters in the nozzle sized by the RG model, we will find an increase in Ma_E compared to that desired in the design by the RG model, and in particular a difference of all parameters, given the difference in the size of the nozzle of the two models.

Now if one uses the present RG model to calculate the flow in the nozzle sized on the basis of the HT or the PG model, the gas will find a reduced space which will influence the behavior of gases and an oblique shock waves will be appear in the nozzle despite the fact that the nozzle is adapted in the direction of HT or PG. Then we will notice that the adaptation of the nozzle actually will be for a large NPR enough compared to that found by the HT and PG models, and this will give us an increase of the zone of the side loads paining with considerable amplitude. So as a solution, it is necessary to respect properly the behavior of the gas during the flow by taking into account good hypotheses bringing the maximum possible towards the reality.

In the international community, the design results given by our RG model cannot currently be verified by existing CFD codes, as they are developed on the basis of consideration of the PG state equation, and not on the consideration of the hypotheses of a real gas. The only way is the verification by wind tunnel experimentation.

Figs.5—8 show the variation of the design parameters L/λ, C_{Mass}, C_F and A_E/A_* as a function of P_0 for the PG, HT and RG models. The presentation is made for air when Ma_E=3.00. For HT and RG models, T_0=2 000 K is taken.

For the PG model the presentation is made for γ=1.402. Note that the PG and HT models do not depend on P_0. The influence of P_0 is noticed in the real case when the effect of the thermal and caloric

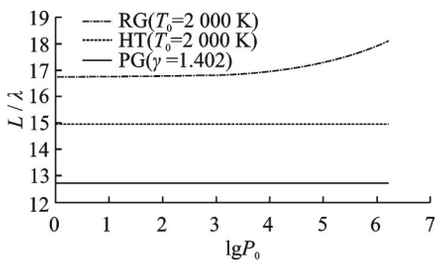

Fig.5 Variation of L/λ versus P_0(Ma_E=3.00)

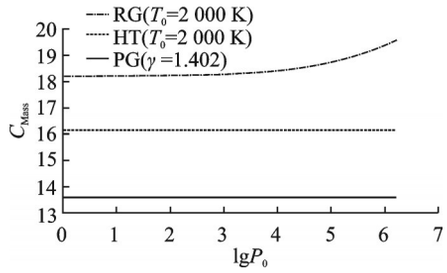

Fig.6 Variation of C_{Mass} versus P_0(Ma_E=3.00)

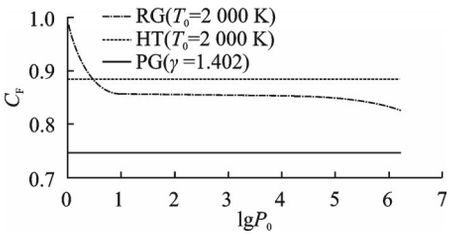

Fig.7 Variation of C_F versus P_0(Ma_E=3.00)

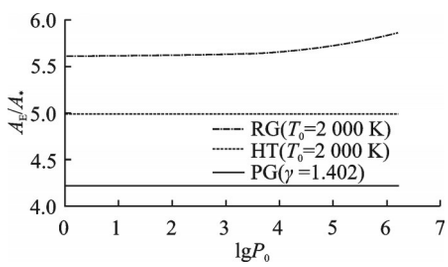

Fig.8 Variation of A_E/A_* versus P_0(Ma_E=3.00)

imperfection is taken into account by the consideration of the real gas model. For the length (Fig.5), C_{Mass} (Fig.6) and A_E/A_* (Fig.8), we note that the size of the nozzle given by the RG model is quite considerable compared to that given by the models PG and HT. For the model RG, the C_F (Fig.7) is lower than that given by the HT model which returns to the distribution of the pressure through the wall of the nozzle.

4.2 Effect of Ma_E on the design parameters

Fig.9 show the effect of Ma_E on the shape of the two-dimensional PN, determined by our RG model when T_0=2 000 K and P_0=50 bar, respectively. The example taken is for Ma_E=2.00, 3.00, 4.00 and 5.00. The design results in the RG framework are shown in the Table 3. For comparison purposes, only the numerical design results of the same nozzles in the HT model[6-7] are presented in Table 4, and the design results for PG model[1-5] are shown in Table 5. It should be noted that the shape of the nozzles given by the PG and HT models are different from those presented in Fig.9. It is clearly noticed again the effect of Ma_E on the PN shape. What disrupts the Ma_E is also an important parameter for our RG model.

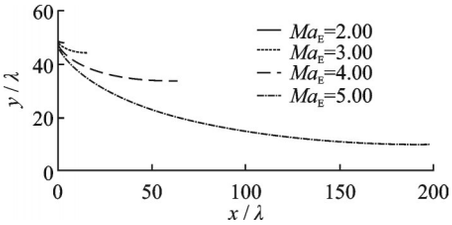

Fig.9 Ma_E effect on the RG two-dimensional PN design (T_0=2 000 K, P_0=50 bar)

Table 3 RG design values for the nozzles in Fig.9

N	Ma_E	L/λ	C_{Mass}	C_F	A_E/A_*
1	2.00	3.772	3.969	0.331	1.867
2	3.00	16.888	18.339	0.850	5.608
3	4.00	64.484	68.922	1.240	16.007
4	5.00	199.162	208.903	1.490	39.035

Table 4 HT design values for the nozzles in Fig.9[6-7]

N	Ma_E	L/λ	C_{Mass}	C_F	A_E/A_*
1	2.00	3.546	3.706	0.331	1.770
2	3.00	14.494	16.142	0.884	4.995
3	4.00	54.640	58.301	1.327	13.861
4	5.00	165.433	173.504	1.630	33.565

Table 5 PG design values for the nozzles in Fig.9[1-5]

N	Ma_E	L/λ	C_{Mass}	C_F	A_E/A_*
1	2.00	3.363	3.494	0.286	1.685
2	3.00	12.698	13.594	0.746	4.220
3	4.00	42.146	44.784	1.127	10.647
4	5.00	122.220	127.979	1.408	24.749

Note in Fig.9 and Tables 3, 4, 5, that according to the variation of Ma_E, the design results given by the RG model are all superior to the design results given by the HT model, and results of both models are superior to the results of PG model. Then the PG and HT models make a default design of the nozzle that will influence the flow quality and the physical interpretation of actual flow behavior.

Figs. 10—13 show the variation of design parameters L/λ, C_{Mass}, C_F and A_E/A_* as a function of Ma_E for the three models PG, HT and our RG. The presentation is made for the air when T_0=2 000 K.

For the model RG we take the example for P_0=50 bar. For the PG model the presentation is

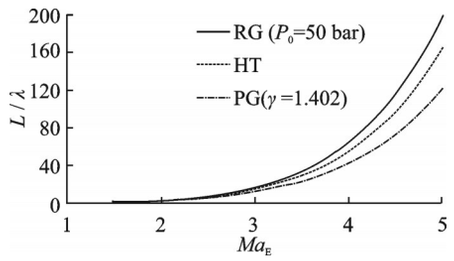

Fig.10 Variation of L/λ versus Ma_E(T_0=2 000 K)

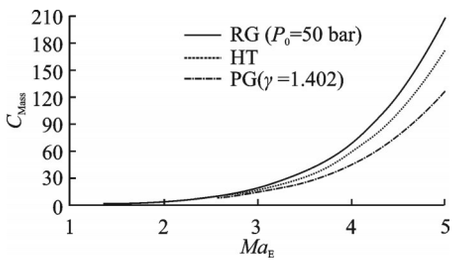

Fig.11 Variation of C_{Mass} versus Ma_E(T_0=2 000 K)

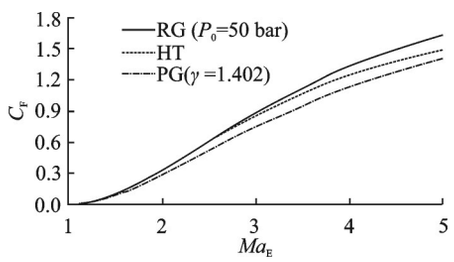

Fig.12 Variation of C_F versus Ma_E(T_0=2 000 K)

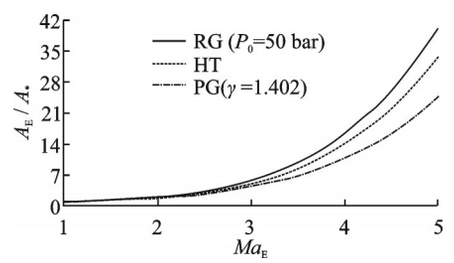

Fig.13 Variation of A_E/A_* versus Ma_E(T_0=2 000 K)

made for γ=1.402. Note that the results given by the RG model is different to that given by the PG and HT models, justified by the influence of P_0 on the design parameters, when the effect of the thermal and caloric imperfection are held in account by the consideration of RG.

4.3 Effect of T_0 on the design parameters

Fig.14 show the effect of T_0 on the shape of the two-dimensional PN, determined by our RG model when P_0=50 bar and Ma_E=3.00 ,respectively. The example taken is for T_0=500 K, 1 000 K, 2 000 K, and 3000 K. The numerical design results in the context of real gas are presented in Table 6. For comparison purpose, we add only the numerical design

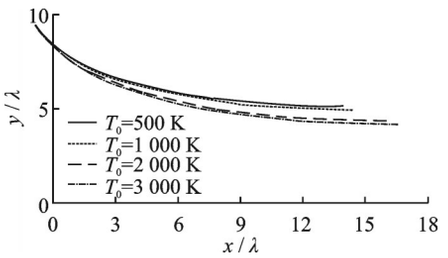

Fig.14 T_0 effect on the RG two-dimensional PN design (Ma_E=3.00, P_0=50 bar)

results of the same nozzles in the framework of HT model[6-7], as presented in Table 7, and the design results in the framework of PG model[1-5], as presented in Table 8. It should be noted that the nozzle shape given by the PG and HT models are different from those presented in Fig.6. It is clearly noticed again the effect of T_0 on the PN shape. What disrupts is that T_0 is also an important parameter in our RG model. It should be noted again that the RG model for high T_0 is different than the results given by the HT model of Refs.[6-7].

Table 6 RG design values for the nozzles in Fig.14

N	T_0/K	L/λ	C_{Mass}	C_F	A_E/A_*
1	500	14.805	15.934	0.703	4.784
2	1 000	15.228	16.445	0.755	4.992
3	2 000	16.888	18.339	0.850	5.608
4	3 000	17.445	18.974	0.881	5.818

Table 7 HT design values for the nozzles in Fig.14[6]

N	T_0/K	L/λ	C_{Mass}	C_F	A_E/A_*
1	500	12.749	13.653	0.750	4.237
2	1 000	13.432	14.427	0.796	4.471
3	2 000	14.949	16.142	0.884	4.995
4	3 000	15.558	16.830	0.918	5.207

Table 8 PG design values for the nozzles in Fig.14[3]

N	γ	L/λ	C_{Mass}	C_F	A_E/A_*
1	1.402	12.698	13.594	0.746	4.220

It is noted in Fig.14 and Tables 6, 7, 8 that according to the variation of T_0, the design results given by the RG model are all superior to the design results given by the HT model, and results of both models are superior to the results of PG model. Then the PG and HT models make a default design of the nozzle that will influence the flow quality, and the physical interpretation of actual flow behavior.

For the PG model, the design results do not

depend on T_0 and P_0. For this reason we find only a value of each parameter according to the value of γ witch is taken to $\gamma=1.402$, as presented in Table 8.

For each parameter of our five design parameters, the RG results are found different from the HT and PG results due to the fact that the P_0 is taken into account in our RG model.

Figs. 15—18 show the variation of design parameters L/λ, C_{Mass}, C_F and A_E/A_* as a function of T_0 for the three PG, HT and RG models. The presentation is made for air when $Ma_E=3.00$. For the RG model, we take the example for $P_0=50$ bar. For the PG model, the presentation is made for $\gamma=1.402$. The PG model does not depend on T_0. Note that the results given by the RG model is different to that given by the two PG and HT models, justified by the influence of P_0 on the design parameters, when the effect of the thermal and caloric imperfection are held in account by the consideration of RG.

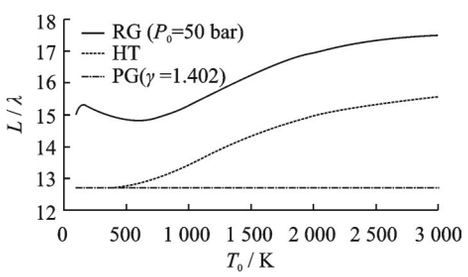

Fig.15 Variation of L/λ versus T_0($Ma_E=3.00$)

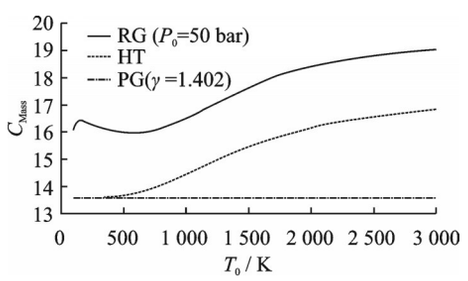

Fig.16 Variation of C_{Mass} versus T_0($Ma_E=3.00$)

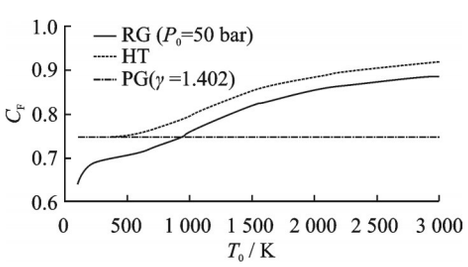

Fig.17 Variation of C_F versus T_0($Ma_E=3.00$)

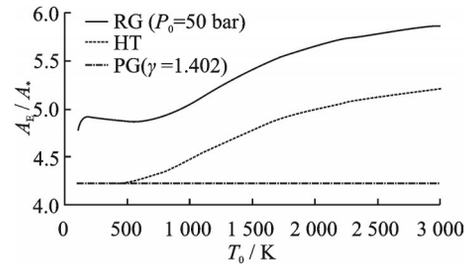

Fig.18 Variation of A_E/A_* versus T_0($Ma_E=3.00$)

5 Conclusions

This work enables us to develop a new model based on the RG assumptions by adding the stagnation pressure P_0 effect on the design of the two-dimensional N. The Berthelot state equation is used for application. The following conclusions are obtained:

(1) The precision of the design parameters depends on the number of the descending Mach lines from the lip.

(2) P_0 is an important parameter for our RG model.

(3) The value of P_0 increases the size of the nozzle compared to those given by the old HT and PG models. Therefore all design parameters also increase with P_0.

(4) The numerical results is controlled by the convergence of A_E/A_* calculated numerically by Eq.(13) towards Eq.(10).

(5) The computer execution time for RG model is quite large compared to that given by the PG and HT models.

(6) For given Ma_E, T_0, λ, infinity of contours can be found by varying P_0.

(7) For the PG and HT models, all the physical parameters can be obtained as a function of one state variable Ma or T. For our RG model, all the physical parameters depend on two state variables T and ρ.

(8) The PG and HT models become a particular case of our RG model.

(9) The Berthelot state equation is taken for our presented RG model.

(10) The nozzle's truncation in the vicinity of the exit section becomes necessary to gain a nozzle mass and length. In parallel, small loss in C_F is obtained.

(11) The error of the PG and HT models can

achieve to 40% and 18%, respectively, compared to our RG model. These errors vary with P_0, T_0 and Ma_E.

We will develop a CFD calculation code based on the consideration of a real gas assumption in order to verify the presented design calculation in future work.

References

[1] ANGELINO G. Approximate method for plug nozzle design[J]. AIAA Journal, 1964, 2(1): 1834-1835.

[2] BERMAN K. The plug nozzle: A new approach to engine design[J]. Astronautics, 1960, 7(1): 22-24.

[3] GREER H. Rapid method for plug nozzle design[J]. ARS Journal, 1961, 31(4): 560-561.

[4] RAO G V R. Spike nozzle contour for optimum thrust[J]. Planetary and Space Science, 1961, 4: 92-101.

[5] ZEBBICHE T. Supersonic plug nozzle design[C]// Proceedings of the 41st AIAA/ASME/SAE/ASEE Joint Propulsion Conference & Exhibi. Tucson, USA: AIAA, 2005.

[6] ZEBBICHE T, YOUBI Z. Supersonic plug nozzle design at high temperature. Application for air[C]//Proceedings of 44th Aerospace Sciences Meeting and Exhibit. Reno Hilton, USA: AIAA, 2006.

[7] ZEBBICHE T, YOUBI Z. Effect of stagnation temperature on the supersonic two-dimensional plug nozzle conception application for air[J]. Chinese Journal of Aeronautics, 2007, 20(1): 15-28.

[8] ZEBBICHE T, YOUBI Z. Effect of stagnation temperature on the supersonic flow parameters with application for air in nozzles[J]. The Aeronautical Journal, 2007, 111(1115): 31-40.

[9] ZEBBICHE T. Stagnation temperature effect on the Prandtl Meyer function[J]. AIAA Journal, 2007, 45(4): 952-954.

[10] ZEBBICHE T, BOUN-JAD M. Numerical quadrature for the Prandtl Meyer function at high temperature with application for air[J]. Thermophysics and Aeromechanics, 2012, 19(3): 381-384.

[11] ONOFRI M. CFD results of plug nozzle test cases [C]//Proceedings of the 38th AIAA/ASME/ SAE/ ASEE Joint Propulsion Conference and Exhibit. Indianapolis, USA: AIAA, 2002.

[12] ROMMEL T, HAGEMANN G, SCHLEY C A. et al. Plug nozzle flow field analysis[J]. Journal of Propulsion and Power, 1997, 13(5): 629-634.

[13] JUNWEI L, YU L, YUNFEI L, et al. Experimental and numerical study on two dimensional plug nozzle [C]//Proceedings of the 46th AIAA/ASME/SAE/ ASEE Joint Propulsion Conference & Exhibit. [S.l.]: AIAA, 2010.

[14] OSLUND J, DAMAGAAD T, FREY M. Side-load phenomena in highly over-expanded rocket nozzle[J]. Journal of Propulsion and Power, 2004, 20(4): 695-704.

[15] RALF H, CHLOE G. Experimental study on rocket nozzle side load reduction[J]. Journal of Propulsion and Power, 2011, 28(2): 307-311.

[16] STARK R, CHLOE G. Optimization of a rocket nozzle side load reduction device[J]. Journal of Propulsion and Power, 2016, 32(6): 1395-1402.

[17] SALHI M, ZEBBICHE T, MEHALEM A. Stagnation pressure effect on Prandtl Meyer function for air[J]. Journal of Aerospace Engineering, 2016, 231(2): 326-337.

[18] SALHI M, ZEBBICHE T, ROUDANE M. Gaseous imperfections effects on the Prandtl Meyer function with application for air[C]//Proceedings of The International Conference on Engineering & Technology. Antalya, Turkey: [s.n.], 2017.

[19] SALHI M, ZEBBICHE T. Gaseous imperfections effect on the supersonic flow parameters for air in nozzles[C]//Proceedings of the 3rd International Conference and Exhibition on Mechanical &Aerospace Engineering. San Francisco, USA:[s.n.], 2015.

[20] SALHI M, ZEBBICHE T, MEHALEM A. Stagnation pressure effect on the supersonic flow parameters with application for air in nozzles[J]. The Aeronautical Journal, 2016, 120(1224): 313-354.

[21] PETERSON C R, HILL P G. Mechanics and thermodynamics of propulsion[M]. New York, USA: Addition-Wesley Publishing Company Inc, 1965.

[22] ZEBBICHE T. Stagnation pressure effect on the supersonic minimum length nozzle design[J]. The Aeronautical Journal, 2019, 123(1265): 1013-1031.

[23] ZEBBICHE T, YOUBI Z. Supersonic two-dimensional minimum length nozzle design at high temperature. application for air[J]. Chinese Journal of Aeronautics, 2007, 20(1): 29-39.

[24] ZEBBICHE T. Stagnation temperature effect on the supersonic axisymmetric minimum length nozzle design with application for air[J]. Advances in Space Research, 2011, 48(22): 1656-1675.

[25] VAN WYLEN G J. Fundamentals of classical thermodynamics[M].[S.l.]: John Wiley and Sons Inc, 1973.

[26] ANNAMALAI K, ISHWAR K P, MILIND A J. Advanced thermodynamics engineering[M]. 2nd Edition. [S.l.]: Taylor and Francis Group, 2011.

[27] RALTSON A, RABINOWITZ A. A first course in numerical analysis[M]. [S. l.]: McGraw Hill Book Company, 1985.

[28] YAHIAOUI T, ZEBBICHE T. Fast algorithm for the inverse of the real gas Prandtl-Meyer function[J]. Journal of the Chinese Society of Mechanical Engineers, 2021,42(3): 325-330.

Authors Dr. **HAMAIDIA Walid** obtained the diplomas of state engineer, magister and diploma of doctorate in Aeronautics from the University of Blida 1 in Algeria. He is currently a researcher at the Higher School of Aeronautical Techniques in Algeria with the rank of Associate Professor. He is very interested in the design of supersonic nozzles, in CFD calculation in nozzles, and in the numerical modeling of supersonic flows.

Prof. **ZEBBICHE Toufik** obtained the doctorate of state degree in Aeronautics from the Institute of Aeronautics and Space Studies at the University of Blida 1 in Algeria and the rank of full professor at this institute. He has published around fifty international publications in renowned impact factor journals and around fifty international conferences. He is invited to several international conferences as a technical program committee member and speakers. He is very interested in several current topics such as the design of the supersonic nozzles by the method of characteristics and CFD calculations, transonic, supersonic and hypersonic flows, wavesshock, generationmesh, vibration of structures applied to nozzles supersonic.

Author contributions Dr. **HAMAIDIA Walid** designed the study, provided data, compared the three models, conducted the analysis, interpreted the results, wrote the manuscript, and commented to the reviewer's comments. Prof. **YAHIAOUI Toufik** provided a data model and mathematical components, supervising the paper, wrote the numerical program interpreted the results, wrote the manuscript, and commented to the reviewers comments and the revised paper. Prof. **ZEBBICHE Toufik** introduced the idea presented in the article, provided data for analysis and background of the study, supervised the paper, wrote the numerical program interpreted the results, wrote the manuscript, and responded to the comments of the reviewers and the revised paper. All three authors developed the numerical calculation program, extracted all results, commented on the draft manuscript and approved the submission.

Competing interests The authors declare no competing interests.

(Production Editor: ZHANG Bei)

停滞压力对超声速二维塞式喷嘴设计的影响

HAMAIDIA Walid[1], *YAHIAOUI Toufik*[2], *ZEBBICHE Toufik*[2]

(1. Higher School of Aeronautical Techniques, Dar elbeida, Algiers, Algeria;
2. Institute of Aeronautics and Space Studies, University of Blida 1, BP 270 Blida 09000, Algeria)

摘要:提出了一种新的计算模型用于研究在出口处存在均匀和平行的气流下,燃烧室的停滞压力对超声速二维塞式喷嘴设计的影响。该模型基于真实气体(Real gas, RG)模型,通过使用Berthelot状态方程,考虑了共体积和分子间的相互作用效应。该模型还考虑了分子振动效应,以评估气体在高温下的行为。停滞压力和停滞温度是模型中的重要参数。在边缘,温度和密度是由2个非线性代数方程的分辨率给出的,这些方程由4个复数函数的积分制定。这是由一个新的、强大的和快速的算法完成的,且其他参数由分析关系决定。喷嘴中的气流扩展是Prandtl Meyer型的。喷嘴轮廓通过将喷嘴边缘的膨胀区离散为几个点来确定。马赫数、流动偏差、压力、温度和密度参数是在反演双变量Prandtl Meyer函数后确定的。计算中提出的函数的积分是由30阶的Gauss Legendre求积获得。由于进口和出口部分的气流是单向的,通过计算临界截面比与理论得到的临界截面比的收敛来进行数值控制并验证结果。在这种情况下,喷嘴的轮廓和流动参数,如喷嘴的质量、长度和推力系数,会自动收敛到精确结果。本文提出的新RG模型是对理想气体(Perfect gas, PG)和高温(High temperature, HT)两种模型的概括。后者可以针对低停滞压力进行设计,并不提供任何关于停滞压力变化的信息。因此,如果后者很高,就有必要通过本文的RG模型来修正PG和HT模型所给出的结果。与其他现有的喷嘴,如最小长度喷嘴(Minimum length nozzle, MLN),相比,塞式喷嘴具有更好的性能和设计参数。将本文RG模型应用到空气气流计算中,可对PG和HT模型的塞式喷嘴的质量、长度和推力系数进行校正。

关键字:Berthelot 状态方程; Gauss Legendre 求积; 喷嘴质量; 最小长度喷嘴; 塞式喷嘴; Prandtl Meyer 函数; 真实气体; 停滞压力; 停滞气温